Low-Distortion Signal Generation for ADC Testing

Fumitaka Abe, Yutaro Kobayashi, Kenji Sawada, Keisuke Kato, Osamu Kobayashi †, Haruo Kobayashi

Division of Electronics and Informatics, Gunma University, Kiryu, Gunma 376-8515 Japan
† Semiconductor Technology Academic Research Center (STARC), Yokohama 222-0033 Japan

Abstract — This paper describes a method of generating low-distortion sinusoidal waves using an arbitrary waveform generator (AWG), and experimental results of using such a generator for ADC dynamic performance testing. With this proposed method, 3rd order harmonics of the generated signal are suppressed simply by changing the AWG program (or waveform memory contents)—AWG nonlinearity identification is not required—and spurious components, generated far from the signal band, are relatively easy to remove using an analog filter; our theoretical analyses, simulations, and experiments showed that a simple passive LC analog filter (with relaxed requirements compared to the one for direct HD3 removal) is sufficient. Our ADC testing results—using signals generated by an AWG with the proposed algorithm, and a simple passive LC LPF—show measurement errors (caused by 3rd order harmonics generated by AWG DAC nonlinearity) half that of previous algorithms.

Keywords — ADC testing, Low distortion signal generation, Arbitrary waveform generator, Third-order harmonics

1. Introduction

LSI production testing is becoming increasingly important in the semiconductor industry, because LSI testing costs are increasing while the cost of silicon is decreasing. ADCs are particularly important key components in mixed-signal SoCs, and here we consider testing of such ADCs, especially dynamic performance testing.

Automatic Test Equipment (ATE) is rather expensive, so semiconductor manufacturers tend to use the same ATE for years. However device under test (DUT) performance is improving rapidly, so it is important to be able to precisely test or measure the performance of future DUTs using today's (relatively low performance) ATE.

An AWG consists of a DSP (or waveform memory) and a DAC. We can use AWGs to generate arbitrary analog waveforms simply by changing the DSP program, and many ATEs use AWGs for their flexibility. However, due to AWG nonlinearities, sinusoidal signals generated by AWGs include harmonics that degrade the accuracy of ADC testing when AWGs are used as ADC input signal sources.

The purpose of this paper is to validate in depth—experimentally and theoretically—the effectiveness of our method [1][2] for generating low-distortion (especially low 3rd harmonic distortion) signals simply by changing the AWG program, without AWG nonlinearity identification, as well as to measure the improvement in accuracy of ADC linearity testing when using the AWG signals as inputs to ADCs.

We also explain how to apply our proposed low distortion signals to ADC output 3rd harmonic measurement. We have found by theoretical analyses, simulations, and experiments that the 3rd order distortion of an ADC under test is NOT measured accurately if the phase-switching technique described below is used to apply signals directly to the ADC, because 3rd order harmonics of the ADC are cancelled at the ADC output. However we show by theoretical analyses, simulations, and experiments that this problem can be solved just by using a simple passive LPF with relaxed requirements compared to the one for direct HD3 removal. Test results for our ADC (12bit SAR ADC, AD7356, 6 samples) using signals generated by an AWG (Agilent 33220A) with our proposed algorithm and a simple passive LC LPF show that errors in 3rd order harmonic measurements due to ADC nonlinearity are half that for previous algorithms.

Our phase-switching technique is explained in Section 2, and the ADC testing conditions are discussed in Section 3. Experimental results are presented in Section 4, and the key points of our work are summarized in Section 5. Appendices I, II, and III show some more theoretical analyses and simulation results.

Note that in this paper, we have described theoretical analyses, simulation, and experiments covering both AWG signal generation and ADC testing. The previous works in [1-5] considered only AWG signal generation, and not ADC testing using the generated signals; In other words, this paper describes problems for ADC testing with the proposed signal generation [1] and its countermeasures. Another low distortion sine signal generation method using an AWG, proposed in [6], requires precise identification of nonlinearity, which our method does not require. Similar techniques for canceling harmonics in power amplifiers, proposed in [7], cannot be applied to the AWG without hardware modification.

2. Test signal generation for ADC testing

2.1 Conventional test signal generation

We consider the case that 3rd order distortion is dominant in the AWG, whose internal DAC has 3rd order distortion. We use a simple model as follows:

$$A_{out}\left(nT_{s(AWG)}\right) = a_1 D_{in}(n) + a_3 D_{in}(n)^3. \quad (1)$$

A conventional ADC test signal generated in the DSP is a sinusoidal signal expressed in equation (2). However the output of the AWG includes 3rd order harmonics because the DAC in the AWG has 3rd order distortion characteristics. Fig.1 shows this conventional test signal generation.

$$D_{in}(n) = X(n) = A \cdot \cos\left(2\pi f_{in} n T_{s(AWG)}\right). \quad (2)$$

978-1-4799-4722-5/14/$31.00 ©2014 IEEE

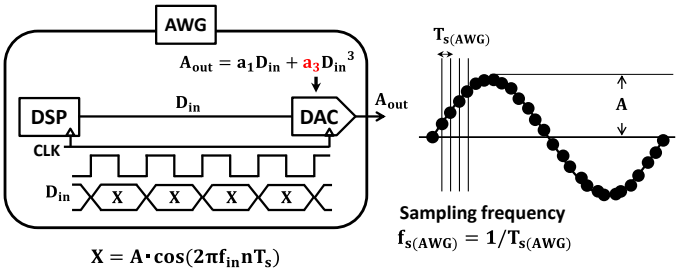

Fig.1 Conventional method of sinusoidal signal generation using an AWG.

2.2 Low-distortion signal generation with phase switching

We consider the case that 3rd order distortion as per equation (1) is dominant in the AWG. We use the same AWG, but change the DSP program as per equation (3) below to cancel the 3rd harmonics caused by the 3rd order nonlinear term [1][2].

$$D_{in}(n) = \begin{cases} X_0(n) = 1.15A \cdot \cos(2\pi f_{in} n T_{s(AWG)} - \dfrac{\pi}{6}) \\ X_1(n) = 1.15A \cdot \cos(2\pi f_{in} n T_{s(AWG)} + \dfrac{\pi}{6}). \end{cases} \quad (3)$$

Here, $X_0(n)$ is used when n is an even number, also $X_1(n)$ is used when n is an odd number. X_0 and X_1 have the same frequency but they differ in phase by $\pi/3$.

We call the signal generated by the algorithm in equation (3) a phase-switching signal (Fig.2). The DSP output signal D_{in} consists of X_0 and X_1, and interleaves them every one clock cycle. This signal configuration cancels 3rd order harmonics caused by the following DAC:

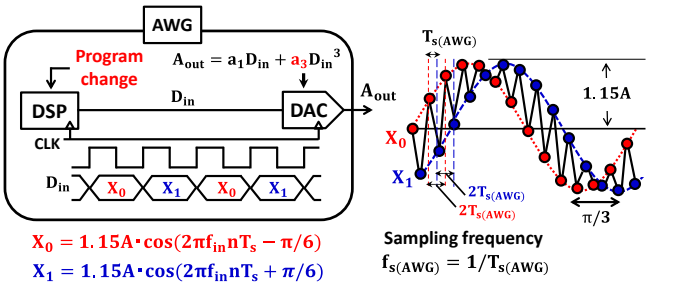

Fig.2 A phase-switching sinusoidal wave generation technique.

We have to set the amplitude of the phase-switching signal 1.15 times larger than for the conventional method so that the fundamental power of the phase-switching signal is equal to that for the conventional method. (However, as explained later, if a simple analog LPF is employed, the amplitude of the phase-switching signal needs to be only 2% larger.) Fig.3 shows both conventional and phase-switching D_{in} spectrums; we see that the phase-switching signal fundamental power is equal to that for the conventional case, and phase-switching causes spurious signals at $f_{s(AWG)}/2 - f_{in}$ whose power is 4.8dB lower than that of the fundamental.

Our simulations and experiments for the phase-switching technique in Fig.3 showed the 3rd order harmonics cancellation effect not only for the DAC in the AWG but also for the ADC under test. Namely, the conditions for cancelling 3rd order harmonics caused by ADC 3rd order distortion are shown in (a) and (b) as follows:

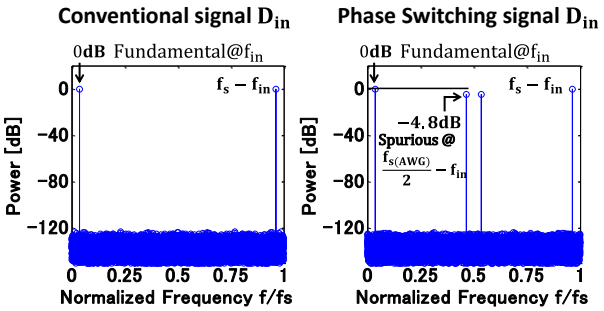

Fig.3 Spectrums for conventional and phase-switching signals Din from DSP or waveform memory AWGs.

Conditions:

(a) Spurious@$\left(\frac{f_{s(AWG)}}{2} - f_{in}\right)$ generation

(b) $\left(\text{Spurious@}\frac{f_{s(AWG)}}{2} - f_{in}\text{ power}\right) -$ (Fundamental Wave@f_{in} power) $= -4.8$dB.

In this case the 3rd order distortion of the ADC cannot be measured because it is cancelled at the ADC output, and in the following sections we will describe countermeasures.

2.3 Test signal generation with an AWG (Agilent 33220A)

Our experiments showed the effectiveness of our "phase-switching" 3rd order harmonic reduction technique for sinusoidal signal generation. Fig.4 and Fig.5 show that for $f_{in} = 200kH$, $f_{s(AWG)} = 10MHz$, the phase-switching signal reduces the power of the 3rd harmonic at 600kHz, but generates a spurious signal at $f_{s(AWG)}/2 - f_{in}$; in other words, the spurious signal at $f_{s(AWG)}/2 - f_{in}$ suppresses the 3rd order harmonics. We call this function *distortion shaping* [1][2], which is similar to but different from noise shaping; that is, 3rd order harmonics near the signal band (which may be difficult to remove with an LPF) are suppressed, while spurious signals are generated far from the signal band (and are relatively easy to attenuate with an LPF).

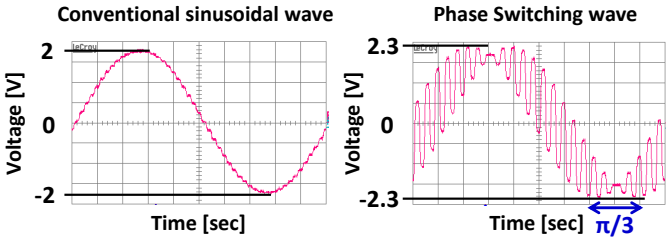

Fig.4 Output signal waveforms of conventional and phase-switching signals generated by Agilent 33220A.

Complete cancellation is not realized in Fig.5 with the phase-switching technique; this is because one of the cancellation conditions of (a), (b) is not completely satisfied.

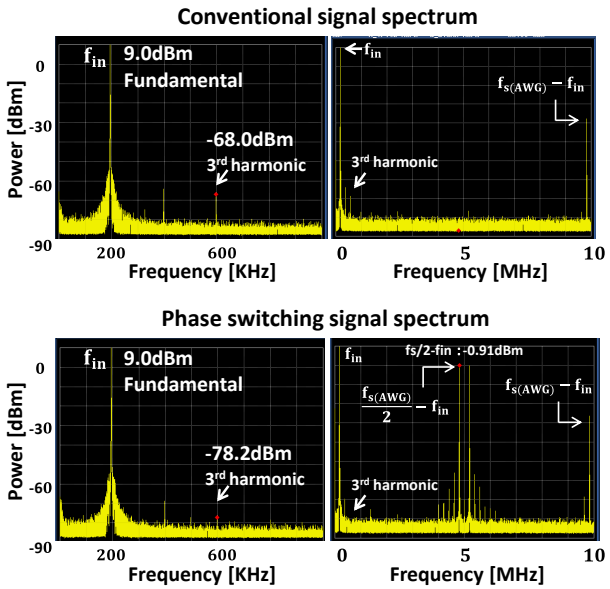

Fig.5 Output signal spectrums of conventional and phase-switching signals generated by Agilent 33220A.

2.4 3rd order harmonic cancellation principle

Here we show that why the 3rd order harmonics caused by the AWG are suppressed by the phase-switching technique [1][2]. Actually both conventional and phase-switching techniques generate 3rd order harmonics due to AWG 3rd order distortion, and their phases are multiplied by 3. Then the phase difference of $\pi/3$ between X_0 and X_1 changes the phase difference between X_0' and X_1' by π; and as a result the 3rd order terms X_0' and X_1' are cancelled. Fig.6 shows the 3rd order harmonic generation and cancellation mechanisms.

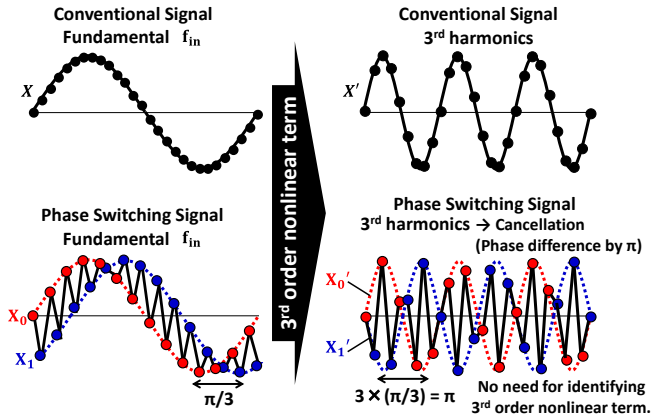

Fig.6 Principle of 3rd order harmonic cancellation using the phase-switching technique.

2.5 Limitations of the phase-switching technique

The phase-switching technique uses two sinusoidal waves shown in equation (3) and Fig.2. On the other hand, the conventional signal is one sinusoidal signal (equation (2) and Fig.1). Thus the number of sampling points per one sinusoidal signal period included in the phase-switching is half that for conventional sinusoidal signals; as a result, the phase-switching sampling frequency is equivalently reduced by half. For this reason, by Shannon's sampling theorem, for the phase-switching technique the range of acceptable sinusoidal wave frequencies for f_{in} is half that for the conventional sinusoidal input.

The other limitation is that this technique is only adequate for low frequencies but hard to realize in mid and high frequencies due to the challenge of getting the fine time resolution to sample the sine wave and the shifted sine wave at the same time.

3. Required conditions for phase-switching spurious signals for ADC dynamic performance testing

3.1 Measurement of 3rd harmonics caused by ADC nonlinearity

We here consider ADC dynamic performance testing—measurement of the level of 3rd order harmonics in the ADC output signal—using the proposed phase-switching signal. This phase-switching signal includes only a low level of 3rd harmonics (Fig.3), so the 3rd order harmonics in the ADC output signal are mainly due to ADC 3rd order distortion. However the phase-switching spurious at $f_{s(AWG)}/2 - f_{in}$ is also inputted to the ADC under test, and thus we have to consider its influence.

Remember that the spurious at $f_{s(AWG)}/2 - f_{in}$ has a 3rd order harmonic suppression effect. When the phase-switching signal including spurious at $f_{s(AWG)}/2 - f_{in}$ is also inputted to an ADC, its output signal may be lower than the actual 3rd order harmonics power, because this spurious at $f_{s(AWG)}/2 - f_{in}$ suppresses 3rd order harmonics caused by the 3rd order distortion of the ADC; hence in this case the 3rd order nonlinearity of the ADC can NOT be measured accurately.

Here we introduce two desirable conditions for accurate 3rd order harmonic measurement with the phase-switching signal.

Conditions:

(c) $\left(\frac{f_{s(AWG)}}{2} - f_{in}\right) > \frac{f_{s(ADC)}}{2}$

(d) Spurious@$\left(\frac{f_{s(AWG)}}{2} - f_{in}\right)$ attenuation by 8 dB (or more).

When conditions (c) and/or (d) are satisfied, accurate 3rd order harmonic measurement with the phase-switching signal is possible. It is desirable to satisfy both, but satisfying even only one makes measurement more accurate.

$f_{s(AWG)}$ and $f_{s(ADC)}$ are sampling frequencies of the AWG and ADC respectively, while f_{in} is the frequency of the sinusoidal wave generated by the AWG. Actually satisfying both conditions (c) and (d) is not difficult; regarding condition (c), $f_{s(AWG)}$ is usually higher than $f_{s(ADC)}$, and ADC testing systems have an analog LPF for anti-aliasing. This LPF may be sufficient to satisfy the above condition (d). The spurious at $f_{s(AWG)}/2 - f_{in}$ is relatively easy to suppress with the LFP because it is very far from the signal band.

First we will explain condition (c). If this condition is satisfied, the sampling theorem says that the phase-switching spurious at $f_{s(AWG)}/2 - f_{in}$ is not reproduced. So the phase-switching spurious at $f_{s(AWG)}/2 - f_{in}$ which has a cancellation effect is moved due to aliasing (Fig.7). We can assume that under condition (c) the phase-switching signal after sampling does not have the cancellation effect because the spurious does not exist at $f_{s(AWG)}/2 - f_{in}$. Condition (a), one of the cancellation conditions, is not satisfied by condition (c).

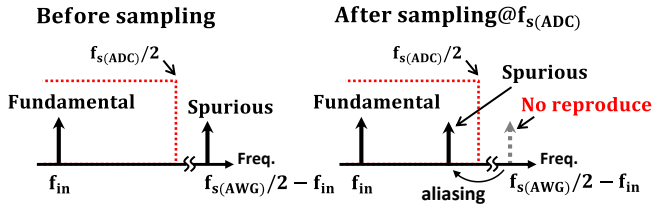

Fig.7 Phase-switching signal spurious @ $f_{s(AWG)}/2-f_{in}$ is moved by the sampling theorem under condition (c).

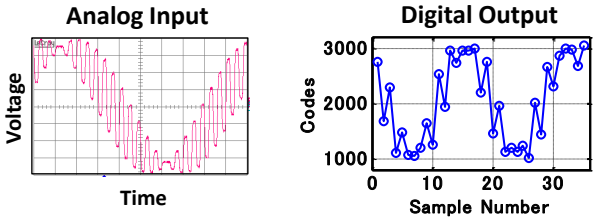

Fig.8 ADC input and output waveforms under condition (c).

Furthermore, Fig.8 shows the input and output waveforms of an ADC with $f_{s(AWG)} = 10MHz$, $f_{in} = 200kHz$ and $f_{s(ADC)} = 3.478261MHz$. We see that the input and output waveforms are not equal because the spurious at $f_{s(AWG)}/2-f_{in}$ is not reproduced; the cancellation effect of the phase difference π in Fig.6 does not occur inside the ADC. In other words, we can accurately measure 3rd order harmonics caused by ADC 3rd order distortion.

Next we will explain condition (d). Notice that both conditions (b) and (d) are not satisfied simultaneously. We have simulated and obtained the correlation between the spurious power at $f_{s(AWG)}/2-f_{in}$ and 3rd order harmonic power. We show the simulation conditions and results in Fig.9 and Fig.10 respectively.

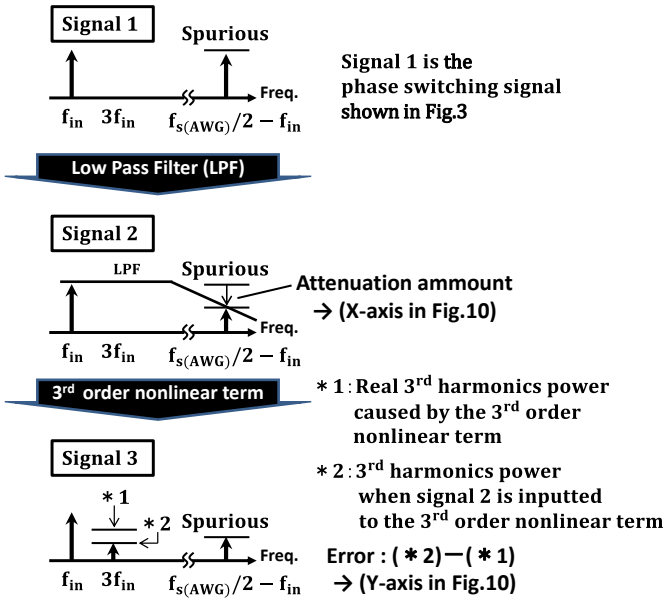

Fig.9 Simulation conditions for calculating attenuation of spurious at $f_{s(AWG)}/2-f_{in}$ and 3rd order harmonic measurement error.

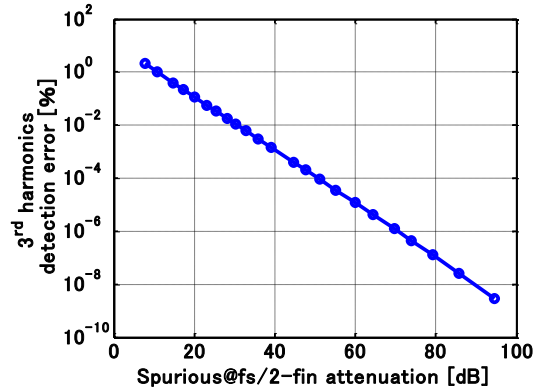

Fig.10 Correlation between spurious power at $f_{s(AWG)}/2-f_{in}$ and 3rd harmonic power measurement error. Simulation results of Fig.9.

We see in Fig.10 that attenuation of the spurious at $f_{s(AWG)}/2-f_{in}$ by 10dB, 20dB and 30dB leads to 3rd harmonic measurement errors of 1%, 0.1% and 0.01% respectively. This error can be significantly further decreased by satisfying condition (c) as well.

As described above, by satisfying both conditions (c) and (d), the 3rd order harmonic measurement error is less than 1%. It is expected that the arguments of this section also hold for IMD3 measurement of two-tone signal generation with the phase-switching technique [3][4]. See appendix III.

3.2 Phase-switching signal amplitude

We have set the amplitude of the phase-switching signal 15% larger than for the conventional signal in order to make the fundamental power equal to that in the conventional case. This over-amplitude of 15% can be reduced by attenuating spurious at $f_{s(AWG)}/2-f_{in}$. Fig.11 shows the correlation between spurious at $f_{s(AWG)}/2-f_{in}$ attenuation level and phase-switching signal amplitude. Fig.11 shows that the phase-switching amplitude error is about 3% when the spurious at $f_{s(AWG)}/2-f_{in}$ is attenuated by 10dB. We see in Fig.11 that with sufficient attenuation of the spurious at $f_{s(AWG)}/2-f_{in}$, this converges to the conventional signal amplitude.

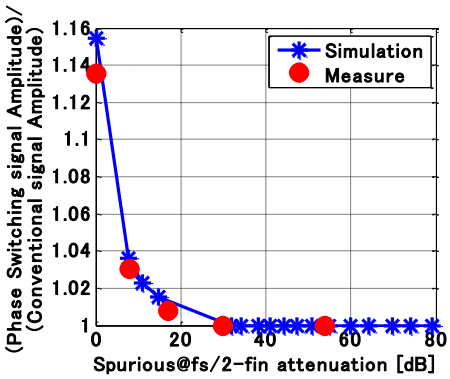

Fig.11 By attenuating the spurious, phase-switching signal amplitude approaches the conventional signal amplitude.

Also, we see in Fig.12 that for the phase-switching signal, sufficient attenuation of the spurious at $f_{s(AWG)}/2-f_{in}$ results in convergence to the conventional signal amplitude and waveform.

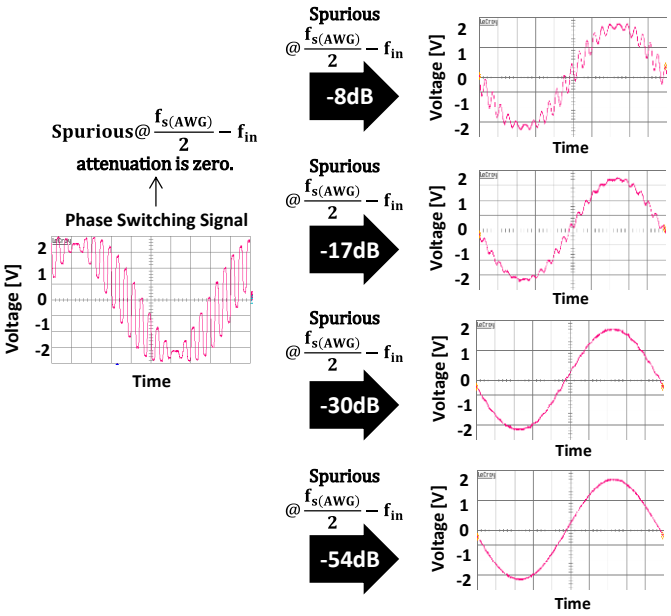

Fig.12 Attenuation of phase-switching signal spurious at $f_{s(AWG)}/2 - f_{in}$

4. ADC dynamic performance testing

We have performed experiments with 12-bit SAR ADCs (AD7356, produced by Analog Devices Inc.). We have measured 3rd order harmonics included in the output of the AD7356 ADCs. The ADC input signals are generated by the conventional and phase-switching techniques shown in Fig.4 and Fig.5. Here, the testing conditions are $f_{s(AWG)} = 10MHz$, $f_{in} = 200kHz$, $f_{s(ADC)} = 3.478261MHz$; these parameters satisfy the condition (c). Also we use LPFs as pre-stage circuit of AD7356. Fig.13 shows the frequency characteristics of the LPFs measured by a Frequency Response Analyzer (NF Corporation FRA). We use a 5th order LC Butterworth LPF with cutoff frequency of fc=250kHz for attenuating 3rd order harmonics generated by Agilent 33220A (AWG). So, we can measure actual 3rd order harmonics generated by AD7356 (ADC) by using this LPF. 4th order LC Butterworth LPFs with several cut off frequencies are used for attenuating the phase-switching spurious at $f_{s(AWG)}/2 - f_{in}$. By using fc=1MHz, 2MHz, 2.7MHz, 3.7MHz, attenuation of spurious at $f_{s(AWG)}/2 - f_{in}$(4.8MHz) changes by 54dB, 30dB, 17dB and 8dB respectively as shown in Fig.13.

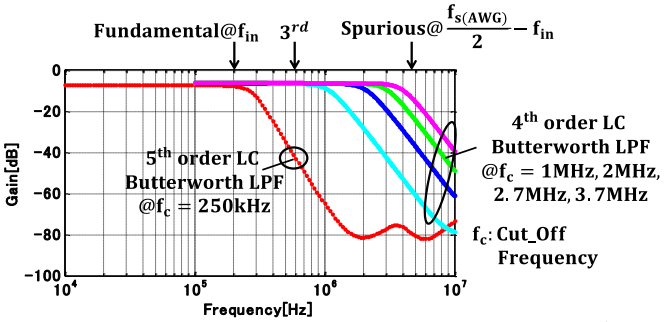

Fig.13 Frequency characteristics of LPFs to attenuate 3rd order harmonics generated by an AWG for ADC testing, and phase-switching spurious @$f_{s(AWG)}/2 - f_{in}$

We have measured 6 samples of AD7356 ADCs, and we observe their spectrums in Fig.14, Fig.15, and Fig.16. Fig.14 shows the case of a conventional signal with a 5th order LPF with fc=250kHz; the measured 3rd order harmonics in Fig.14 are actual 3rd order harmonics caused by AD7356 3rd order distortion. We consider this data (-94.6dBFs) as the reference.

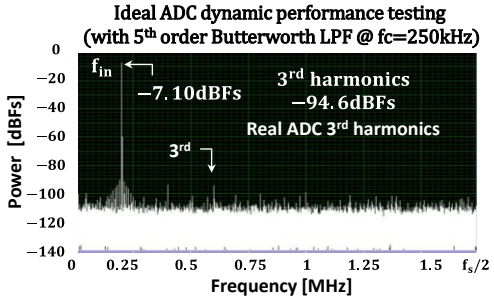

Fig.14 Output signal power spectrum of AD7356 using a conventional signal input with a 5th order LPF @fc=250MHz (that is, a very low distortion sinusoidal signal).

Fig.15 shows the case using the conventional signal input with a 4th order LFP @fc = 1MHz, where the 3rd order harmonic power is -88.5dBFs (fundamental wave power is -6.94dBFs). Considering that the actual 3rd order harmonic power is -94.6dBFs in Fig.14, the measurement error is estimated as 6.5%. On the other hand, Fig.16 shows the case using the phase-switching signal input with a 4th order LPF @fc=1MHz, where the 3rd harmonic power is -92.6dBFs (fundamental wave power is -7.09dBFs); the measurement error is 2.1%.

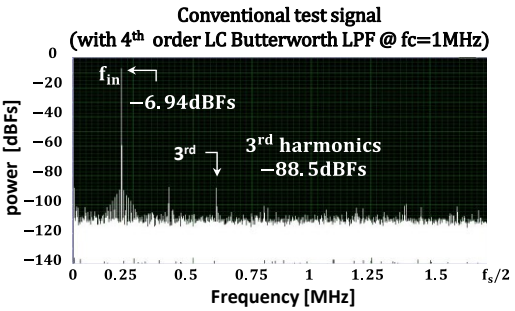

Fig.15 Output signal power spectrum of AD7356 using a conventional signal input with a 4th order LPF @fc=1MHz.

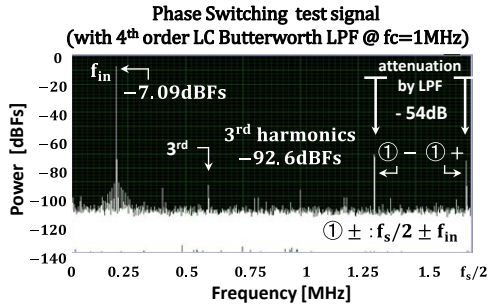

Fig.16 Output signal power spectrum of AD7356 using a phase-switching signal input with a 4th order LPF @fc=1MHz.

In the same way we have measured and calculated 3rd harmonic measurement error of AD7356 for all 6 samples. Fig.17 shows the measurement results, where a "minus"

measurement error means that 3rd order harmonics are lower than the reference, while a "plus" measurement error means that 3rd order harmonics are higher than the reference. Note that a "plus" measurement error is physically reasonable; when it approaches zero, the testing quality is good. On the other hand, a "minus" measurement error is not acceptable; this is due to using the phase-switching technique without an LPF (the ADC 3rd order distortion of the DUT is cancelled). We also confirmed this effect by simulation.

AD7356 (ADCs) 3rd order harmonic measurement accuracy is improved by using a phase-switching signal with a LPF for all 6 samples, which validates the effectiveness of our proposed technique. However, we have to consider the measurement results in Fig.17. For both the conventional method and phase-switching technique, the measurement error characteristic is almost flat between 8dB spurious at $f_{s(AWG)}/2 - f_{in}$ attenuation and 54dB. This means that attenuation of the spurious at $f_{s(AWG)}/2 - f_{in}$ by 8dB is sufficient for measuring 3rd order harmonics generated by AD7356. So, we see that our phase-switching technique improves 3rd harmonic measurement accuracy by satisfying both conditions (c) and (d). However when just condition (a) is satisfied (that is, attenuation of spurious at $f_{s(AWG)}/2 - f_{in}$ is zero), 3rd order harmonics caused by AD7356 are not measured accurately (results are smaller than actual harmonics) as per the data for sample 3 shown in Fig.17.

Sample 3 has "minus" error @ 0dB attenuation. This means that ADC performance looks very good. Also, Sample 5 shows zero error @ 0dB attenuation. However, this is also strange because with phase switching there are small amounts of 3rd harmonics but not zero. Therefore we have to attenuate spurious at $f_{s(AWG)}/2 - f_{in}$ by about 8 dB to measure 3rd order harmonics of ADCs. The measurement errors coverage to some small value by attenuating spurious at $f_{s(AWG)}/2 - f_{in}$.

5. Conclusion

This paper has described a low-distortion sinusoidal wave generation method with an AWG and experimental verification using it for ADC dynamic performance testing. We have the following observations:

1) With the proposed method, 3rd order harmonics are attenuated just by changing the program or waveform memory contents of the AWG.
2) Nonlinearity identification for the DAC inside the AWG is not required.
3) We found that if the signal generated by the proposed phase switching algorithm without a LPF is directly applied to an ADC, its output signal does not contain the harmonics caused by ADC nonlinearity (the harmonics are cancelled); the ADC linearity cannot be tested accurately.
4) However, by attenuating the spurious at fs/2 – fin by 8 dB (or more) with a simple analog LPF: by using a simple analog LPF the harmonics caused by ADC non-linearity appear at the ADC output; its linearity can be tested with the signal generated by the proposed method.
5) The fundamental power of the sinusoidal signal generated by the proposed method without an analog LPF is attenuated by 15%; this may affect testing of the input dynamic range of the ADC under test. However, when an analog LPF as described in 4) is employed, it is attenuated only by 2% and hence this is not a problem.
6) The maximum frequency generated by the proposed method is half that of conventional methods using an AWG with given sampling frequency fs. However, the rapid advancement of LSI technology means that DAC (AWG) sampling speed are increasing, but device mismatches (which cause DAC nonlinearity) are not improving, hence the proposed approach will be even more cost effective as LSI technology progresses in future.
7) All of the above arguments were verified by experiments using the AWG (Agilent 33220A) and 6 samples of 12bit SAR ADCs (AD7356); the 3rd order harmonic measurement error is reduced by approximately half.
8) ADC BIST research has been active such as [8, 9], though its practical application in industry is still controversial. If the proposed phase-switching method were used (with an on-chip DAC and LPF) to generate the sinusoidal signals for the on-chip ADC testing, this would relax the LPF requirements and so facilitate ADC BIST implementation.

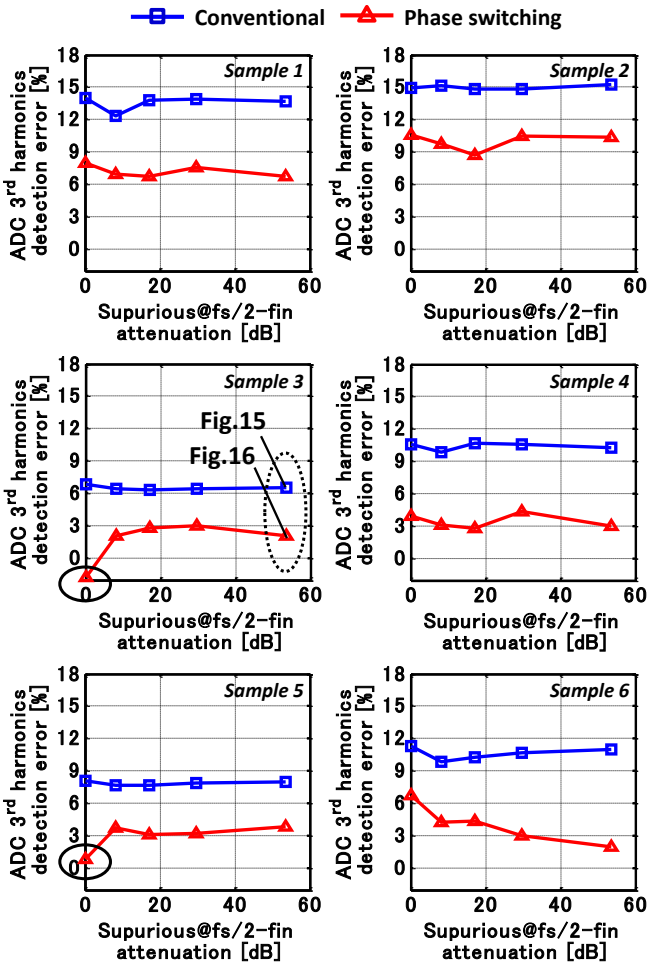

Fig.17 3rd order harmonic measurement errors for AD7356.

We have proposed and investigated a low-distortion signal generation method with an AWG for ADC testing [1, 2], and the contents described here demonstrate their effectiveness for practical use with experiments through AWG signal generation to ADC testing.

We close this paper by remarking that we have also proposed and investigated the following signal generation methods with simulations and experiments [1-5], and we

expect that combining these algorithms with a simple analog LPF or BPF would improve ADC linearity testing quality:

a) Low-distortion sinusoidal signal generation algorithms with techniques such as 2nd order harmonic cancellation, or both 3rd and 5th order harmonic cancellation [1, 2].
b) Two-tone signal generation algorithms with low IMD3 using an AWG for telecommunication-use ADCs [3, 4].
c) Application of these algorithms to a delta-sigma DAC as well as to a Nyquist-rate DAC.

According to our simulations and theoretical analysis, we have found that similar arguments hold in the above cases a), b) and c), and hence the proposed approach here seems valid in more general cases. Some results are shown in appendices II and III. We hope to report more details of this investigation elsewhere.

Acknowledgements

We would like to thank S. Shibuya, T. Arafune, S. Sasaki, M. Higashino, T. Matsuura, M. Tsuji, M. Watanabe, N. Dobashi, S. Umeda, R. Shiota, N. Kiichi, N. Takai, T. J. Yamaguchi, T. Arakawa,T. Ensaka, K. Katoh and K. Wilkinson.

REFERENCES

[1] K. Wakabayashi, K. Kato, T. Yamada, O. Kobayashi, H. Kobayashi, F. Abe, K. Niitsu,"Low-Distortion Sinewave Generation Method Using Arbitrary Waveform Generator", J. of Electronic Testing, Theory and Applications, Springer, vol.28, Issue. 5, pp. 641-651 (Oct. 2012).

[2] K. Wakabayashi, T. Yamada, S. Uemori, O. Kobayashi, K. Kato, H. Kobayashi, K. Niitsu, H. Miyashita, S. Kishigami, K. Rikino, Y. Yano, T. Gake, "Low-Distortion Single-Tone and Two-Tone Sinewave Generation Algorithms Using an Arbitrary Waveform Generator", IEEE International Mixed-Signals, Sensors, and Systems Test Workshop, Santa Barbara, CA (May 2011).

[3] K. Kato, F. Abe, K. Wakabayashi, C. Gao, T. Yamada, H. Kobayashi, O. Kobayashi, K. Niitsu, "Two-Tone Signal Generation for Communication Application ADC Testing", IEEE Asian Test Symposium, Niigata, Japan (Nov. 2012).

[4] K. Kato, F. Abe, K. Wakabayashi, C. Gao, T. Yamada, H. Kobayashi, O. Kobayashi, K. Niitsu, "Two-Tone Signal Generation for ADC Testing," IEICE Trans. on Electronics, vol.E96-C, no.6, pp.850-858 (June 2013).

[5] T. Yamada, O. Kobayashi, K. Kato, K. Wakabayashi, H. Kobayashi, T. Matsuura, Y. Yano, T. Gake, K. Niitsu, N. Takai, T. J. Yamaguchi, "Low-Distortion Single-Tone and Two-Tone Sinewave Generation Using ΣΔ DAC", IEEE International Test Conference (poster session), Anaheim, CA (Sept. 2011)

[6] A. Maeda, "A Method to Generate a Very Low Distortion High Frequency Sine Wave Using an AWG," IEEE International Test Conference, Santa Clara, CA (2008).

[7] R. Shrestha, E. Mensink, E. A. M. Klumperink, G. J. M, Wienk, B. Nauta, "A Multi-Path Technique Canceling Harmonics and Sidebands in a Wideband Power Upconverter," IEEE International Solid-State Circuits Conference, San Francisco, CA (2006).

[8] W. Jiang, D. Agrawal, "Built-in Self-Calibration of On-chip DAC and ADC," IEEE International Test Conference, Santra Clara, CA (Oct. 2008).

[9] B. Mullane, V. O'Brien, C. MacNamee, T. Fleischmann, "A2D Test: A Complete Integrated Solution for On-Chip ADC Self-Test and Analysis," IEEE International Test Conference, Austin, TX (Nov. 2009).

Appendix I

This appendix I shows analytically that ADC 3rd-order distortion cannot be measured directly if a phase-switching signal is used (due to 3rd-order harmonic cancellation), but it can be measured if condition (d) in Sec. 2.5 above is satisfied.

Recall eq.(1) and AWG output can be written as follows.

$$\mathrm{Y}(\mathrm{n}T_s) = a_1 D_{in}(n) + a_3\{D_{in}(n)\}^3$$

We use Din in eq.(3), and the AWG output is calculated as follows [1]:

$$\begin{aligned}\mathrm{Y}(\mathrm{n}T_s) &= a_1 D_{in}(n) + a_3\{D_{in}(n)\}^3 \\ &= \mathrm{P}\sin(2\pi f_{in} n T_s) \\ &\quad + \mathrm{Q}\cos\left(2\pi\left(\frac{f_s}{2} - f_{in}\right)nT_s\right) \\ &\quad + \mathrm{R}\cos\left(2\pi(\frac{f_s}{2} - 3f_{in})nT_s\right).\end{aligned}$$

Here

$$\begin{aligned}\mathrm{P} &\equiv \frac{\sqrt{3}}{2}\left(a_1 A + \frac{3}{4}a_3 A^3\right) \\ \mathrm{Q} &\equiv \frac{1}{2}\left(a_1 A + \frac{3}{4}a_3 A^3\right) \\ \mathrm{R} &\equiv -\frac{1}{4}a_3 A^3.\end{aligned}$$

Next we consider the case that an analog LPF following the AWG attenuates $\left(\frac{f_s}{2} - f_{in}\right)$ component by α and $(\frac{f_s}{2} - 3f_{in})$ component by β , and then we obtain the ADC input as follows:

$$\begin{aligned}&\mathrm{Y}(\mathrm{n}T_s) = \frac{\sqrt{3}}{2}\left(a_1 A + \frac{3}{4}a_3 A^3\right)\sin(2\pi f_{in} n T_s) \\ &+ \frac{1}{2}\cdot\alpha\cdot\left(a_1 A + \frac{3}{4}a_3 A^3\right)\cos\left(2\pi(\frac{f_s}{2} - f_{in})nT_s\right) \\ &- \frac{1}{4}\cdot\beta\cdot a_3 A^3\cos\left(2\pi(\frac{f_s}{2} - 3f_{in})nT_s\right).\end{aligned}$$

We assume here fs(AWG) = fs(ADC) for simplicity, and we model the ADC under test as follows:

$$\mathrm{Z}(\mathrm{n}T_s) = b_1 Y(nT_s) + b_3\{Y(nT_s)\}^3.$$

Then the ADC output can be calculated as follows:

$$\begin{aligned}\mathbf{Z}(\mathbf{n}T_s) &= \left\{b_1 P + b_3\left(\frac{3}{4}P^3 + \frac{3}{2}\alpha^2 PQ^2 + \frac{3}{2}\beta^2 PR^2 - \frac{3}{2}\alpha\beta PQR\right)\right\}\sin(2\pi f_{in} n T_s) \\ &+ b_3\left(-\frac{1}{4}P^3 + \frac{3}{2}\alpha\beta PQR\right)\sin(2\pi 3 f_{in} n T_s) \\ &+ \left\{b_1\alpha Q + b_3\left(\frac{3}{4}\alpha^3 Q^3 + \frac{3}{2}\alpha P^2 Q - \frac{3}{4}\beta P^2 R + \frac{3}{2}\alpha\beta^2 QR^2\right)\right\}\cos\left(2\pi\left(\frac{f_s}{2} - f_{in}\right)nT_s\right) \\ &+ b_3\left(-\frac{3}{4}\alpha P^2 Q + \frac{3}{4}\alpha^2\beta Q^2 R\right)\cos\left(2\pi\left(\frac{f_s}{2} + f_{in}\right)nT_s\right) \\ &+ \left\{b_1\beta R + b_3\left(\frac{3}{4}\beta^3 R^3 - \frac{3}{4}\beta P^2 Q + \frac{3}{2}\beta P^2 R + \frac{3}{2}\alpha^2\beta Q^2 R\right)\right\}\cos\left(2\pi\left(\frac{f_s}{2} - 3f_{in}\right)nT_s\right) \\ &+ b_3\left\{-\frac{3}{4}\beta P^2 R + \frac{3}{4}\alpha\beta^2 QR^2\right\}\cos\left(2\pi\left(\frac{f_s}{2} - 5f_{in}\right)nT_s\right) \\ &+ \frac{3}{4}b_3\alpha^2 PQ^2\sin(2\pi(f_s - f_{in})nT_s) \\ &+ b_3\left\{-\frac{3}{4}\alpha^2 PQ^2 + \frac{3}{2}\alpha\beta PQR\right\}\sin(2\pi(f_s - 3f_{in})nT_s) \\ &+ b_3\left(\frac{3}{4}\beta^2 PR^2 - \frac{3}{2}\alpha\beta PQR\right)\sin(2\pi(f_s - 5f_{in})nT_s) \\ &- \frac{3}{4}b_3\beta^2 PR^2\sin(2\pi(f_s - 7f_{in})nT_s) \\ &+ \frac{1}{4}b_3\alpha^3 Q^3\cos\left(2\pi\left(\frac{3}{2}f_s - 3f_{in}\right)nT_s\right) \\ &+ \frac{3}{4}b_3\alpha^2\beta Q^2 R\cos\left(2\pi\left(\frac{3}{2}f_s - 5f_{in}\right)nT_s\right) \\ &+ \frac{3}{4}b_3\alpha\beta^2 QR^2\cos\left(2\pi\left(\frac{3}{2}f_s - 7f_{in}\right)nT_s\right) \\ &+ \frac{1}{4}b_3\beta^3 R^3\cos\left(2\pi\left(\frac{3}{2}f_s - 9f_{in}\right)nT_s\right).\end{aligned}$$

We see that $\sin(2\pi 3 f_{in} n T_s)$ and $\sin(2\pi(f_s - 3f_{in})nT_s)$ components at the ADC output are cancelled when the phase-switching signal is directly applied (i.e., in case $\boldsymbol{\alpha = 1}$).
Coefficient of $\sin(2\pi 3 f_{in} n T_s)$ is given by

$$b_3\left(-\frac{1}{4}P^3 + \frac{3}{2}\alpha\beta PQR\right).$$

Coefficient of $\sin(2\pi(f_s - 3f_{in})nT_s)$ is given by

$$b_3\left\{-\frac{3}{4}\alpha^2 PQ^2 + \frac{3}{2}\alpha\beta PQR\right\}.$$

Note that

$$\sin(2\pi(f_s - 3f_{in})nT_s) = -\sin(2\pi 3 f_{in} n T_s).$$

Then we merge both terms and the coefficient of the merged $\sin(2\pi 3 f_{in} n T_s)$ term is given by

$$\begin{aligned}
&b_3\left(-\frac{1}{4}P^3 + \frac{3}{2}\alpha\beta PQR\right) - b_3\left\{-\frac{3}{4}\alpha^2 PQ^2 + \frac{3}{2}\alpha\beta PQR\right\} \\
&= b_3\left(-\frac{1}{4}P^3 + \frac{3}{4}\alpha^2 PQ^2\right) \\
&= b_3\left\{-\frac{1}{4}\left(\frac{\sqrt{3}}{2}\left(a_1 A + \frac{3}{4}a_3 A^3\right)\right)^3\right. \\
&\left. + \frac{3}{4}\alpha^2\left(\frac{\sqrt{3}}{2}\left(a_1 A + \frac{3}{4}a_3 A^3\right)\right)\left(\frac{1}{2}\left(a_1 A + \frac{3}{4}a_3 A^3\right)\right)^2\right\} \\
&= b_3\left\{\frac{3\sqrt{3}}{8}\left(a_1 A + \frac{3}{4}a_3 A^3\right)^3\right\}(-1 + \alpha^2) \\
&= -b_3\left\{\frac{3\sqrt{3}}{8}\left(a_1 A + \frac{3}{4}a_3 A^3\right)^3\right\}(1 - \alpha^2).
\end{aligned}$$

With some reasonable assumptions (such as that $\boldsymbol{a_1}$ is dominant compared to $\boldsymbol{a_3}$), we see that if $\boldsymbol{\alpha}$ is somewhat small (say, 0.1), we can accurately measure 3rd order distortion.

Note that coefficient of $\boldsymbol{\sin(2\pi f_{in} n T_s)}$ is given by

$$\begin{aligned}
&\frac{\sqrt{3}}{2}\left(a_1 A + \frac{3}{4}a_3 A^3\right)\left\{b_1 + \frac{3}{16}a_1^2 b_3 A^2\right. \\
&\quad + \frac{3}{16}\left(\frac{3}{2} + \alpha\beta\right)a_1 a_3 b_3 A^4 \\
&\left.\quad + \frac{3}{32}\left(\frac{9}{8} + \beta^2 + \frac{3}{2}\alpha\beta\right)a_3^2 b_3 A^6\right\}.
\end{aligned}$$

Then Fig. 18 shows numerical calculation results (based on the above equations) of the error of

$$\boldsymbol{f_{in}\text{Amplitude} / 3f_{in}\text{ Amplitude}}$$

between the phase switching signal input with attenuation $\boldsymbol{\alpha}$ and the ideal sinusoidal input cases for a1=b1=1, a3=b3=-0.005, $\beta = 1$. We see that when $\boldsymbol{\alpha}$ is small, the error is small.

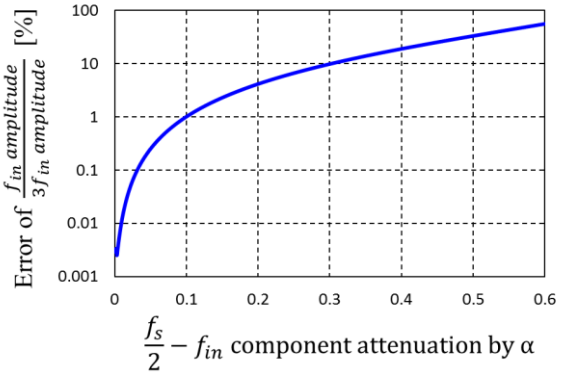

Fig.18 Error of the measurable fundamental and 3rd order harmonic amplitude ratio with the phase switching technique, based on numerical calculation of the above derived equations.

Fig. 19, Fig. 20, and Fig. 21 show ADC test simulation results using a1=b1=1, a3=b3=-0.0101, several input amplitudes and frequencies when not using (LHS figure) or using (RHS figure) an LPF to attenuate high-frequency spurious of the AWG output. The three RHS figures show that 3rd order harmonics can be measured directly when an LPF is used.

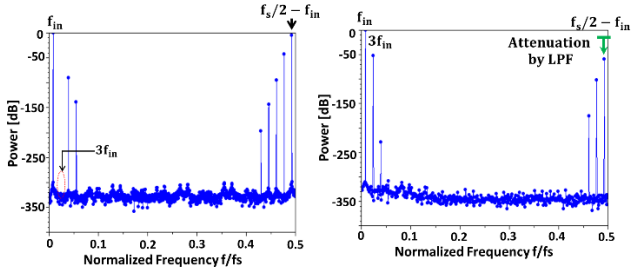

Fig. 19 Power spectrum of ADC output Z(nTs) with the input amplitude A=1, fin/fs= 0.0078125. (Left) No attenuation of high frequency spurious signals. (Right) Attenuation with an LPF (α=0.0019270, β=0.0010991).

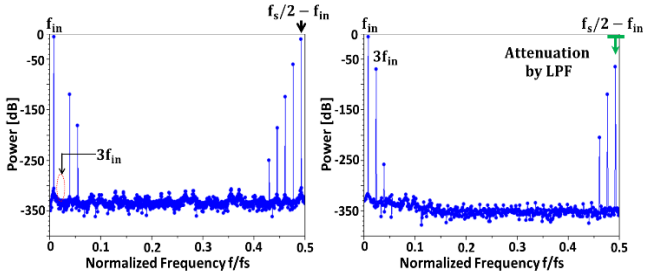

Fig.20 Power spectrum of ADC output Z(nTs) with the input amplitude A=1/2, fin/fs= 0.0078125. (Left) No attenuation of high frequency spurious signals. (Right) Attenuation with an LPF (α=0.0019234, β=0.0011031).

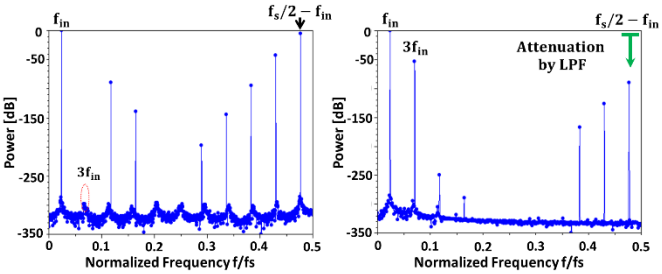

Fig.21 Power spectrum of ADC output Z(nTs) with the input amplitude A=1/2, fin/fs= 0.0234375.(Left) No attenuation of high frequency spurious signals. (Right) Attenuation with an LPF (α=0.0000576, β=0.0000605).

Appendix II

This appendix II shows analytically that ADC 2nd-order distortion cannot be measured directly using a phase-switching signal source with 2nd-order harmonic cancellation [1], but it can be measured if the spurious components at high frequencies are attenuated by even a small amount.

Suppose that an AWG has the second-order harmonics and its output can be written as follows.

$$Y(nT_s) = a_1 D_{in}(n) + a_2\{D_{in}(n)\}^2.$$

Then we use the following Din for the second-order distortion cancellation [1]:

$$D_{in}(n) = \begin{cases} A \cdot \sin(2\pi f_{in} n T_{s(AWG)} - \frac{\pi}{4}) & \text{n: odd} \\ A \cdot \sin\left(2\pi f_{in} n T_{s(AWG)} + \frac{\pi}{4}\right). & \text{n:even} \end{cases}$$

The AWG output is calculated as follows [1]:

$$\begin{aligned} \mathrm{Y}(\mathrm{n}T_s) &= a_1 D_{in}(n) + a_2\{D_{in}(n)\}^2 \\ &= \frac{a_2 A^2}{2} + \frac{\sqrt{2}}{2} a_1 A\cos(2\pi f_{in} n T_s) \\ &+ \frac{\sqrt{2}}{4} a_1 A\cos\left(2\pi\left(\frac{f_s}{2} + f_{in}\right) n T_s\right) \\ &+ \frac{\sqrt{2}}{4} a_1 A\cos\left(2\pi\left(\frac{f_s}{2} - f_{in}\right) n T_s\right) \\ &+ \frac{1}{4} a_2 A^2 \sin\left(2\pi\left(\frac{f_s}{2} + 2f_{in}\right) n T_s\right) \\ &- \frac{1}{4} a_2 A^2 \sin\left(2\pi\left(\frac{f_s}{2} - 2f_{in}\right) n T_s\right). \end{aligned}$$

Next we consider the case that an analog LPF following the AWG attenuates $\left(\frac{f_s}{2} - f_{in}\right)$ component by α, $(\frac{f_s}{2} + 2f_{in})$ component by β, $\left(\frac{f_s}{2} + 2f_{in}\right)$ component by γ and $\left(\frac{f_s}{2} - f_{in}\right)$ component by η (here $0 < \alpha, \beta, \gamma, \eta <= 1$), and we obtain the ADC input as follows:

$$\begin{aligned} \mathrm{Y}(\mathrm{n}T_s) &= a_1 D_{in}(n) + a_2\{D_{in}(n)\}^2 \\ &= \frac{a_2 A^2}{2} + \frac{\sqrt{2}}{2} a_1 A\cos(2\pi f_{in} n T_s) \\ &+ \frac{\sqrt{2}}{4} \cdot \alpha \cdot a_1 A\cos\left(2\pi\left(\frac{f_s}{2} + f_{in}\right) n T_s\right) \\ &+ \frac{\sqrt{2}}{4} \cdot \beta \cdot a_1 A\cos\left(2\pi\left(\frac{f_s}{2} - f_{in}\right) n T_s\right) \\ &+ \frac{1}{4} \cdot \gamma \cdot a_2 A^2 \sin\left(2\pi\left(\frac{f_s}{2} + 2f_{in}\right) n T_s\right) \\ &- \frac{1}{4} \cdot \eta \cdot a_2 A^2 \sin\left(2\pi\left(\frac{f_s}{2} - 2f_{in}\right) n T_s\right). \end{aligned}$$

We assume here $f_{s(AWG)} = f_{s(ADC)}$ for simplicity, and we model the ADC under test which has the second-order distortion as follows:

$$\mathrm{Z}(\mathrm{n}T_s) = b_1 Y(nT_s) + b_2\{Y(nT_s)\}^2.$$

Then the ADC output can be calculated as follows:

Then we have the ADC output as follows:

$$\begin{aligned} Z(nT_s) &= \frac{1}{32} A^2 \Big(16a_2 b_1 + 2a_1^2 b_2(4 + \alpha^2 + \beta^2) \\ &\quad + A^2 a_2^2 b_2(8 + \gamma^2 + \eta^2)\Big) \\ &+ \frac{1}{8} A^2 a_1^2 b_2(-2 + \alpha\beta)\cos(2\pi 2 f_{in} n T_s) \\ &- \frac{1}{16} A^4 a_2^2 b_2 \gamma\eta \cos(2\pi 4 f_{in} n\pi T_s) \\ &+ \frac{1}{16} A^2 a_1^2 b_2 \beta^2 \cos(2\pi(f_s - 2f_{in}) n T_s) \\ &- \frac{1}{32} A^4 a_2^2 b_2 \eta^2 \cos(2\pi(f_s - 4f_{in}) n T_s) \\ &- \frac{A^3 a_1 a_2 b_2 \eta}{4\sqrt{2}} \cos\left(2\pi\left(\frac{f_s}{2} - 3f_{in}\right) n\pi T_s\right) \\ &+ \left(\frac{1}{8} A^2 a_1^2 b_2 \alpha\beta + \frac{1}{16} A^4 a_2^2 b_2 \gamma\eta\right)\cos(2\pi f_s n T_s) \\ &+ \left(\frac{A a_1 b_1 \beta}{2\sqrt{2}} + \frac{A^3 a_1 a_2 b_2 \beta}{2\sqrt{2}} \right. \\ &\quad \left. + \frac{A^3 a_1 a_2 b_2 \eta}{4\sqrt{2}}\right)\cos\left(2\pi\left(\frac{f_s}{2} - f_{in}\right) n T_s\right) \\ &+ \left(\frac{A a_1 b_1 \alpha}{2\sqrt{2}} + \frac{A^3 a_1 a_2 b_2 \alpha}{2\sqrt{2}} \right. \\ &\quad \left. + \frac{A^3 a_1 a_2 b_2 \gamma}{4\sqrt{2}}\right)\cos\left(2\pi\left(\frac{f_s}{2} + f_{in}\right) n T_s\right) \\ &+ \frac{1}{16} A^2 a_1^2 b_2 \alpha^2 \cos(2\pi(f_s + 2f_{in}) n T_s) \\ &- \frac{1}{32} A^4 a_2^2 b_2 \gamma^2 \cos(2\pi(f_s + 4f_{in}) n T_s) \\ &- \frac{A^3 a_1 a_2 b_2 \gamma}{4\sqrt{2}} \cos\left(2\pi\left(\frac{f_s}{2} + 3f_{in}\right) n T_s\right) \\ &+ \frac{1}{32} A\big(16\sqrt{2} a_1 b_1 + 16\sqrt{2} A^2 a_1 a_2 b_2 + 2\sqrt{2} A^2 a_1 a_2 b_2 \beta\gamma \\ &\quad + 2\sqrt{2} A^2 a_1 a_2 b_2 \beta\eta\big)\sin(2\pi f_{in} n T_s) \\ &+ \frac{1}{32} A\big(2\sqrt{2} A^2 a_1 a_2 b_2 \beta\gamma + 2\sqrt{2} A^2 a_1 a_2 b_2 \alpha\eta\big)\sin(2\pi 3 f_{in} n T_s) \\ &- \frac{A^3 a_1 a_2 b_2 \alpha\eta}{8\sqrt{2}} \sin(2\pi(f_s - f_{in}) n T_s) \\ &- \frac{1}{4} A^2 a_1^2 b_2 \beta \sin\left(2\pi\left(\frac{f_s}{2} - 2f_{in}\right) n\pi T_s\right) \\ &+ \frac{1}{32} A(8A a_1^2 b_2 \beta - 8A a_1^2 b_2 \alpha)\sin\left(2\pi \frac{f_s}{2} n T_s\right) \\ &+ \frac{1}{32} A(-8A a_2 b_1 \eta - 8A^3 a_2^2 b_2 \eta)\sin\left(2\pi\left(\frac{f_s}{2} - 2f_{in}\right) n\pi T_s\right) \\ &- \frac{A^3 a_1 a_2 b_2 \beta\eta}{8\sqrt{2}} \sin(2\pi(f_s - 3f_{in}) n T_s) \\ &+ \frac{A^3 a_1 a_2 b_2 \beta\gamma}{8\sqrt{2}} \sin(2\pi(f_s + f_{in}) n T_s) \\ &+ \frac{A^3 a_1 a_2 b_2 \alpha\gamma}{8\sqrt{2}} \sin(2\pi(f_s + 3f_{in}) n T s) \\ &+ \frac{1}{32} A(8A a_1^2 b_2 \alpha + 8A a_2 b_1 \gamma \\ &\quad + 8A^3 a_2^2 b_2 \gamma)\sin\left(2\pi\left(\frac{f_s}{2} + 2f_{in}\right) n T_s\right). \end{aligned}$$

Coefficient of $\cos(2\pi 2 f_{in} n T_s)$ is given by

$$\frac{1}{8} A^2 a_1^2 b_2(-2 + \alpha\beta).$$

Coefficient of $\cos(2\pi(f_s - 2f_{in}) n T_s)$ is given by

$$\frac{1}{16} A^2 a_1^2 b_2 \beta^2.$$

Coefficient of $\cos(2\pi(f_s + 2f_{in}) n T_s)$ given by

$$\frac{1}{16} A^2 a_1^2 b_2 \alpha^2.$$

Note that

$$\cos(2\pi(f_s - 2f_{in}) n T_s) = \cos(2\pi 2 f_{in} n T_s),$$
$$\cos(2\pi(f_s + 2f_{in}) n T_s) = \cos(2\pi 2 f_{in} n T_s).$$

We see that $\cos(2\pi 2 f_{in} n T_s)$ and $\cos(2\pi(f_s \pm 2f_{in}) n T_s)$ components at the ADC output are cancelled when the phase-switching signal is directly applied (i.e., in case $\alpha = \beta = 1$).

Then we merge both terms and the coefficient of the merged $\cos(2\pi 2 f_{in} n T_s)$ term is given by

$$\begin{aligned} &\frac{1}{8} A^2 a_1^2 b_2(-2 + \alpha\beta) + \frac{1}{16} A^2 a_1^2 b_2 \beta^2 + \frac{1}{16} A^2 a_1^2 b_2 \alpha^2 \\ &= \frac{1}{16} a_1^2 b_2 A^2(\alpha^2 + \beta^2 + 2\alpha\beta - 4) \\ &= \frac{1}{16} a_1^2 b_2 A^2\{(\alpha + \beta)^2 - 4\}. \end{aligned}$$

By making some reasonable assumptions (such as $\boldsymbol{a_1}$ is dominant compared to $\boldsymbol{a_2}$) we see that if $\boldsymbol{\alpha + \beta}$ is somewhat small (say, 0.1), we can accurately measure 2nd order distortion.

Note that coefficient of $\boldsymbol{\cos(2\pi f_{in} n T_s)}$ given by

$\frac{\sqrt{2}}{2}a_1A(b_1+a_2b_2A^2)+\frac{\sqrt{2}}{16}a_1a_2b_2A^3(\alpha+\eta)(\beta+\gamma)$.

Fig. 21 shows numerical calculation results (based on the above equations) of the error of

$$f_{in}\textbf{Amplitude}\ /2f_{in}\ \textbf{Amplitude}$$

between the phase switching signal input with attenuation $\boldsymbol{\alpha, \beta}$ and the ideal sinusoidal input cases for a1=b1=1, a3=b3=-0.005, $\boldsymbol{\gamma = \eta = 1}$. We see that when $\boldsymbol{\alpha + \beta}$ is small, the error for HD2 detection is small. In other words, it is useful to use a sinusoidal signal generated by phase switching for ADC second-order distortion testing when its high frequency components are attenuated even by a small amount.

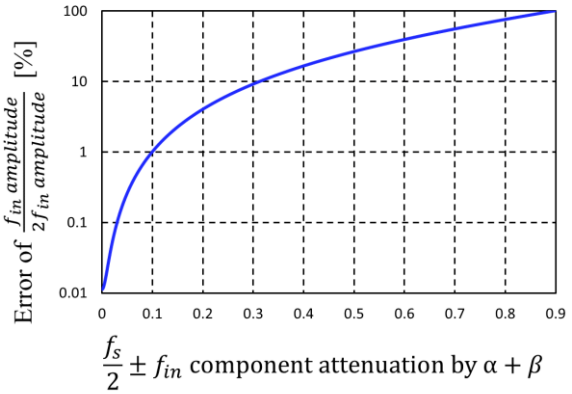

Fig.22 Error of the measurable fundamental and 2nd order harmonic amplitude ratio with the phase switching technique, based on numerical calculation of the above derived equations.

Appendix III

Now let us consider a two-tone signal (f1, f2) generated by phase switching for ADC IMD3 measurement [4, 5]. The analysis is very complicated, so only simulation results are shown here.

Fig. 23 shows the simulated two-tone signal power spectrum generated by phase switching WITHOUT attenuation of high frequency components. We see that the IMD3 components are removed. Fig. 24 shows the ADC output spectrum for the two-tone input signal in Fig.20, and we see that IMD3 components can NOT be measured even if the ADC has third-order distortion.

Fig. 25 shows the two-tone signal power spectrum WITH attenuation of high frequency components. Fig. 26 shows ADC output for the two tone signal in Fig. 25, and we see that IMD3 components can be measured when the ADC has third-order distortion.

Hence the same argument holds for ADC testing using a two-tone signal generated by phase switching. Notice that direct filtering of IMD3 is difficult. However, the phase switching technique is also applicable to two-tone signals and with relaxed filtering of high frequency components of the ADC input (instead of IMD3 filtering), the ADC output IMD3 can be measured correctly.

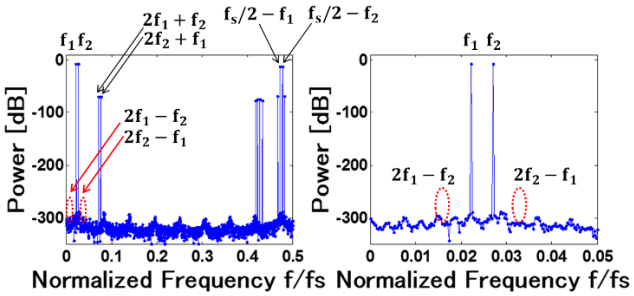

Fig.23 Two-tone signal power spectrum generated by the phase switching technique without attenuation of high frequency components.

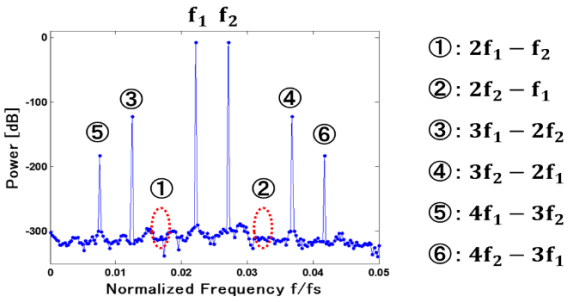

Fig.24 ADC output spectrum for the two-tone input signal in Fig.23. IMD3 components cannot be measured directly even if the ADC has third-order distortion.

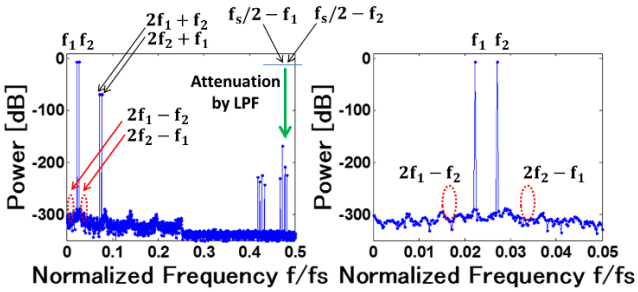

Fig.25 Two-tone signal power spectrum generated by the phase switching technique, and attenuation of high frequency components by the following LPF.

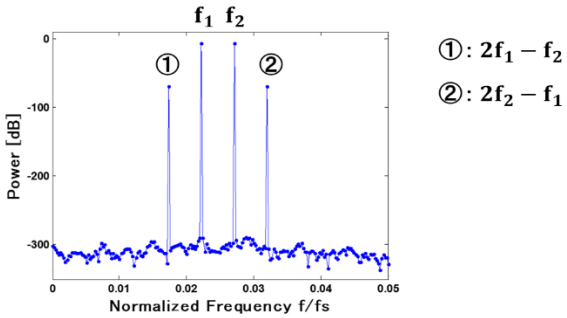

Fig.26 ADC output spectrum for the two-tone input signal in Fig.25. IMD3 components can be measured directly.